

EFFECT OF ALLOYING AND HEAT TREATMENT ON EMBRITTLEMENT OF Fe-Cr-Ni ALLOYS IN HIGH-PRESSURE HYDROGEN

O. I. Balytskyi^{a,b,1} and L. M. Ivaskevych^{a,2}

UDC 620.197:669.788

The nickel content effects on the strength, plasticity, and low-cycle life of hardened and aged specimens of different modifications of austenitic iron-nickel steels and alloys in the initial state and after preliminary high-temperature hydrogenation in hydrogen at a pressure of 30 MPa and temperatures of 293, 773 and 973 K were studied. At 293 K, hydrogen embrittlement of hardened materials weakens with increasing nickel concentration from 10 to 23 wt.%; it is insignificant in the concentration range of 23–45 wt.% and significantly increases with higher nickel content. After aging, materials with a nickel content of 23 and 36 wt.% are insensitive to the action of the hydrogen environment; at higher hydrogen concentrations, embrittlement intensifies. The structural state of aged materials significantly affects the degree of hydrogen embrittlement of their various modifications during short-term tensile tests and slightly less during low-cycle fatigue tests. In the range of Ni concentrations of 23–73 wt.%, the effect of hydrogen on the relative transverse narrowing remains almost stable. The relative elongation of more hydrogen-resistant modifications of materials and low-cycle life increases with increasing nickel content. At 773 K, the effect of nickel content on the relative transverse narrowing in gaseous hydrogen at a pressure of 30 MPa is slightly smaller but qualitatively the same as at 293 K. At 973 K, more heat-resistant high-nickel alloys embrittle in a hydrogen environment much more strongly than hard dispersion steels. Thermomechanical treatment, according to the quenching scheme, tension at room temperature, and aging for 16 h at 973 K significantly increases the plasticity of materials in the presence of hydrogen at the same strength.

Keywords: austenite, intermetallics, hydrogen embrittlement, low-cycle life, strength, plasticity, thermomechanical treatment.

Introduction. The accident-free operation of critical equipment in a number of industries, the working processes of which are characterized by high levels of pressure and temperature of gaseous hydrogen, the tension of structural elements with strict requirements for specific weight indicators, is ensured by the correct choice of structural materials [1–5]. Austenitic iron-nickel steels and alloys are used in aerospace [1–3], chemical and oil and gas [1–4] industries, energy, nuclear and automotive industries [1–3, 5–9] due to the successful combination of operational characteristics in the temperature range from cryogenic to high. Their heat and corrosion resistance is provided by the chromium content of more than 11 wt.%, while high strength and heat resistance – by alloying with intermetallic (Al, Ti, Nb) and refractory (Mo, V, W) metals [6–9]. Depending on the operating temperature and force conditions, such materials contain from 8–10 [8–15] to 80 wt.% Ni [5, 6, 9, 16–26]. To improve the grain boundary

^aKarpenko Physico-Mechanical Institute, National Academy of Sciences of Ukraine, Lviv, Ukraine (balitskii@ipm.lviv.ua). ^bWest Pomeranian University of Technology in Szczecin, Szczecin, Poland (ivaskevich@ipm.lviv.ua). Translated from Problemy Mitsnosti, No. 1, pp. 95 – 107, January – February, 2023. Original article submitted October 20, 2022.

structure and increase resistance to intergranular fracture, B, Zr, Ce, and La are introduced into dispersion-hardening high-nickel alloys [17, 18, 24–31].

The use of iron-nickel steels and alloys in hydrogen energy is limited by the sensitivity of their operational characteristics to hydrogen. It has been established that at room temperature, nickel is an alloying element that determines the surface and diffusion processes of hydrogenation and the hydrogen embrittlement degree of unstable and stable chromium-nickel steels [5, 6, 8–15] and iron-nickel steels and nickel alloys in the hardened state [5–7, 16–30]. Under electrolytic hydrogenation, an adverse effect of nickel on the plasticity of austenitic steels was found. This is caused by a stronger surface cold-hardening of nickel-enriched steels, further reducing the plasticity resource during subsequent mechanical tests [9]. In high-pressure hydrogen gas, nickel significantly improves its hydrogen resistance [5, 8–15]. At the same time, the external hydrogen environment promotes crack initiation and propagation on the surface and reduces tensile plasticity more than the internal pre-absorbed hydrogen [15, 16, 19, 20, 23]. In the range of nickel concentrations from 12.5 to 35% in the hardened state, steels are weakly sensitive to hydrogen, while the influence of minor elements and impurities (Mo, Mn, Ti, and S) is insignificant [5, 9, 15]. The minimum hydrogen embrittlement of binary Fe-Ni alloys was found at 40–50% nickel content, which correlates with their minimum hydrogen permeability [5, 9]. The strength of hardened materials is relatively low; to increase it, aging is carried out, which causes the release of various secondary phases, mainly intermetallics [5, 24–44]. The structure and mechanical properties of steels and alloys after aging often differ significantly, so the effect of nickel content on their hydrogen stability has not been analyzed. Hydrogen diffusion in aged materials is slower than in hardened materials, but the former are more sensitive to hydrogen [29, 30, 32].

The regularities of the effect of electrolytic hydrogenation have been established at room temperature [5, 9, 38, 39] and preliminary high-temperature hydrogenation – at temperatures up to 573 K, when the negative effect of internal hydrogen on the properties of steels and high-nickel alloys is significant [2, 5–7, 15, 35]. Taking into account that embrittlement of such materials was found in the temperature range of 293–1073 K during tests in high-pressure hydrogen gas [11, 19, 20, 23, 29–31, 34], it is crucial to determine the role of nickel at elevated temperatures.

Below are the results of studies of the effect of nickel content on hydrogen embrittlement at temperatures of 293, 773, and 973 K of hardened and aged iron-nickel steels and alloys under the effect of an external hydrogen atmosphere and pre-adsorbed hydrogen.

Materials and Methods. Such alloys as 12Kh18N10T, 10Kh11N23T3MR (EP-33), 10Kh15N27T3V2MR (EP-700) austenitic steels and KhN36TYu (EI-702), KhN45MBTYu (EP-915), KhN55MBYy (EP-666), KhN56MBYuD (EK-62), KhN60MBYy (EP-901), KhN62BMKTYu (EP742), and KhN73MBTYu (EI698) were subjected to short-term tensile and low-cycle fatigue tests. These alloys contained Fe- and Ni-based multicomponent γ -solid solutions with allocated strengthening intermetallic phases and carbides. The content of intermetallics of the type $(\text{Ni,Cr,Fe})_3(\text{Nb,Al,Ti,Mo})$ in aged materials was determined by physicochemical phase analysis in an aqueous electrolyte with ammonium sulfate. Depending on the chemical composition and heat treatment (HT) modes, it varied from 5 to 28 wt.% [11, 18–20, 23, 29–31]. All alloys were subjected to vacuum arc remelting, which provides the formation of structures with thin grain boundaries, reduced amount of carbides and carbonitrides, increased plasticity, fracture toughness, and hydrogen resistance [30].

The results of mechanical tests of modifications of materials with different contents of alloying elements and HT modes are given in [11, 19, 20, 23, 29–31]. One of the variants of chemical composition, HT, and mechanical characteristics at room temperature in air and hydrogen under a pressure of 30 MPa after preliminary hydrogenation is given in Tables 1 and 2. The amount of alloying elements in the modifications of steels and alloys varied within limits provided by regulatory documents. The values of the strength characteristics σ_u and $\sigma_{0.2}$ and plasticity δ and ψ of standard 5-fold cylindrical specimens with a working part diameter of 5 mm were determined at a short-term tensile speed of 0.1 mm/min. The number of cycles to failure N of polished flat specimens with a working part of $3 \times 6 \times 20$ mm under rigid pure zero bending was determined at a strain amplitude of 1.6% and a loading frequency of 0.5 Hz. Such loading conditions make it possible to determine the maximum hydrogen embrittlement of the studied materials [11, 18–20, 23, 29–31].

Since the purity of the hydrogen environment has a significant effect on the mechanical properties [2, 4–6, 29], the specimens were tested in hydrogen with a controlled total oxygen and water vapor content of up to 0.004 g/m³ after double vacuuming of the experimental chamber to a pressure of 0.13 Pa and intermediate flushing with hydrogen. Some specimens were previously kept at 530 K and hydrogen pressure up to 35 MPa for 10 h to compare the effect of pre-absorbed hydrogen and hydrogen atmosphere. Comparative tests were carried out at room temperature in air, while at elevated temperatures – in helium at a pressure of 10 MPa.

TABLE 1. Chemical Composition of the Investigated Materials (wt.%)

| Material | C | Si | Cr | Ni | Mo | W | Fe | Ti | Al | Nb | Others |
|--------------------------|------|------|------|------|------|------|------|------|------|------|---------------------------------------|
| 12Kh18N10T | 0.10 | 0.76 | 17.6 | 10.4 | – | – | 71.2 | 0.96 | – | – | Cu-0.24; Mn-0.22 |
| 05Kh11N23T3MR (EP-33) | 0.05 | 0.37 | 11.4 | 23.2 | 1.48 | – | 59.6 | 2.98 | 0.62 | – | B-0.015; Mn-0.33 |
| 10Kh15N27T3V2MR (EP-700) | 0.09 | 0.60 | 15.0 | 27.1 | 1.41 | 1.92 | 50.8 | 2.85 | 0.29 | – | B-0.002; Co-0.01 |
| KhN36TYu (EI-702) | 0.04 | 0.34 | 12.4 | 36.0 | – | – | 47.0 | 3.04 | 1.15 | – | Mn-0.95 |
| KhN45MTYu (EP-915) | 0.05 | 0.18 | 14.5 | 44.0 | 1.75 | – | 36.6 | 1.67 | 0.5 | 2.7 | Cu-0.02; Zr-0.02; V-0.3 |
| KhN55MBYu (EP-666) | 0.05 | 0.23 | 19.0 | 55.0 | 8.87 | – | 12.0 | – | 1.49 | 1.73 | Se-0.01; Cu-0.02; N-0.07 |
| KHN56MBYuD (EK-62) | 0.04 | 0.12 | 16.7 | 56.2 | 5.24 | – | 14.2 | 0.5 | 1.37 | 3.99 | Cu-0.49; Zr, Ce, La- 0.01 each; V-0.4 |
| KhN60MVYu (EP-901) | 0.02 | 0.16 | 19.3 | 59.7 | 9.12 | 4.83 | 0.54 | – | 2.6 | – | V-6.2 |
| KhN62BMKTYu (EP742) | 0.03 | 0.12 | 13.8 | 62.2 | 5.94 | 0.41 | 0.96 | 2.5 | 2.37 | 3.29 | Co-10.2; B, Zr-0.01, La-0.1 |
| KhN73MBTYu (EI698) | 0.05 | 0.02 | 14.6 | 73.1 | 3.00 | 0.01 | 0.39 | 2.54 | 1.7 | 2.09 | Cu-0.09; Mn-0.11; B, Zr-0.005 |

TABLE 2. Heat Treatment Modes and Mechanical Properties of Alloys at Room Temperature in Air (above the dash) and in Hydrogen at 30 MPa after Preliminary Hydrogenation (below the dash)

| Material | Heat treatment mode | | Mechanical properties | | | | | C _H , mln ⁻¹ |
|-----------------|-----------------------------|--------------------------------|-----------------------|----------------------|-----------------|-----------------|----------------------|------------------------------------|
| | Quenching | Aging | σ_u , MPa | $\sigma_{0.2}$, MPa | δ , % | ψ , % | N cycles to fracture | |
| 12Kh18N10T | 1373 K, 1 h | – | <u>690</u> 680 | <u>310</u> 320 | <u>64</u> 48 | <u>79</u> 55 | <u>1950</u> 750 | 11 |
| 05Kh11N23T3MR | 1373 K, 1 h | 1000 K, 16 h + 923 K, 5 год | <u>1200</u> 1210 | <u>880</u> 880 | <u>29</u> 20 | <u>47</u> 23 | <u>3000</u> 1020 | 15 |
| 10Kh15N27T3V2MR | 1373 K, 1 h | 1023 K, 16 h + 923 K, 10 h | <u>1270</u> 1240 | <u>870</u> 880 | <u>17</u> 10 | <u>23</u> 10 | <u>2277</u> 455 | 15 |
| KhN36TYu | 1210 K, 1 h | 930 K, 4 h | <u>1100</u> 1030 | <u>710</u> 700 | <u>31</u> 14 | <u>52</u> 20 | <u>2680</u> 777 | 18 |
| KhN45MBTYu | 1373 K, 1 h | 1023 K, 10 h + 923 K, 10 h | <u>1160</u> 960 | <u>780</u> 740 | <u>25</u> 4 | <u>38</u> 14 | <u>2560</u> 614 | 19 |
| KhN55MBYu | 1323 K, 1 h | 1000 K, 15 h + 923 K, 10 h | <u>1080</u> 970 | <u>650</u> 660 | <u>35</u> 5 | <u>38</u> 19 | <u>3200</u> 199 | 24 |
| KhN56MBYuD | 1253 K, 1 h | 1003 K, 15 h + 923 K, 10 h | <u>1320</u> 965 | <u>840</u> 750 | <u>34</u> 6 | <u>48</u> 13 | <u>3108</u> 249 | 20 |
| KhN60MVYu | 1423 K, 1 h | 973 K, 10 h + 923 K, 10 h | <u>1170</u> 1070 | <u>810</u> 760 | <u>39</u> 5 | <u>39</u> 15 | – | 23 |
| KhN62BMKTYu | 1343 K, 8 h | 1123 K, 6 h + 1073 K, 13 h | <u>1390</u> 1220 | <u>900</u> 880 | <u>25</u> 4 | <u>29</u> 9 | <u>2998</u> 334 | 29 |
| KhN73MBTYu | 1393 K, 8 h, 1273 K, 4 h | 1048 K, 16 h | <u>1120</u> 1010 | <u>720</u> 690 | <u>31</u> 5 | <u>38</u> 10 | <u>2610</u> 235 | 29 |

The hydrogen content C_H in the specimens after preliminary hydrogenation, determined on the ONH-836, TCH-600 devices by Leco company according to the methods [45, 46], is given in Table 2. The hydrogen embrittlement degree was estimated by the coefficient β , defined as the ratio of the characteristics in hydrogen and vacuum (for example, the coefficient of hydrogen effect on low-cycle life $\beta_N = N_H/N_{He}$).

Results and Discussion. Since the strength characteristics of σ_u and $\sigma_{0.2}$ of 05Kh11N23T3MR and 10Kh15N27T3V2MR steels change insignificantly under the hydrogen effect, and the maximum reduction of σ_u of nickel alloys does not exceed 27% of the values in air, the nickel content effect on the hydrogen embrittlement degree was estimated by the values of plasticity and low-cycle life, which decrease several times (Table 2, Figs. 1–3).

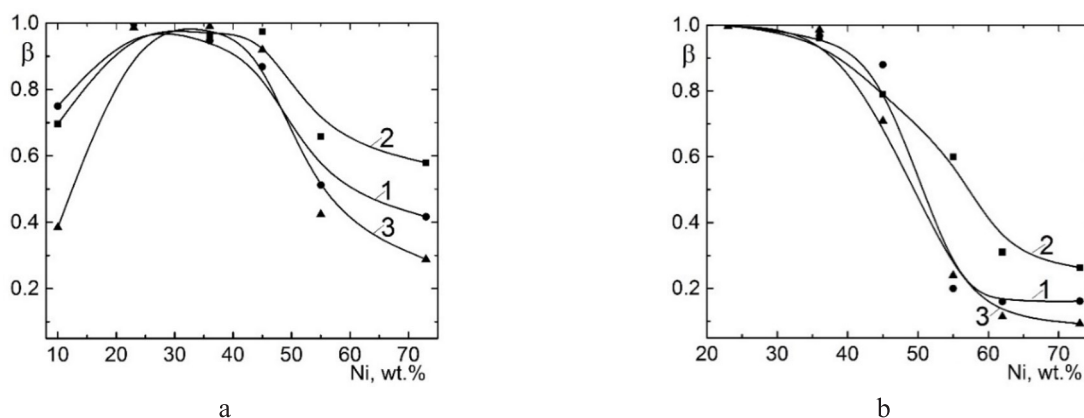


Fig. 1. Dependence of the coefficient of hydrogen influence β at a pressure of 30 MPa on the relative elongation δ (1), transverse narrowing ψ (2), and low-cycle life N (3) of specimens from steels and alloys in the hardened (a) and aged (b) state on the nickel content at room temperature.

Modifications of materials and quenching temperatures of preliminary non-hydrogenated hardened specimens tested in hydrogen at room temperature are given in Tables 1 and 2. In the hardened state, the strength characteristics of the materials differ insignificantly; the short-term strength and yield strength limits are in the range of 600–700 MPa and 290–330 MPa, respectively. A slightly greater difference in the values of plasticity characteristics, relative elongation, and transverse narrowing vary from 45 to 64% and from 55 to 79%. The obtained results (Fig. 1a) are in complete agreement with the available literature data [5–30]. Hydrogen embrittlement of unstable austenitic steels such as 12Kh18N10T is associated with the peculiarities of deformation martensitic transformation under loading in the presence of hydrogen [5, 8–15]. An increase in the energy of packing defects and stabilization of austenite due to an increase in the nickel content from 10 to 23 wt.% lead to the absence of hydrogen effect on the plasticity and low-cycle durability of 05Kh11N23T3MR steel and KhN36TYu alloy (Fig. 1a). The hardened specimens from KhN45MBTYu alloy are slightly embrittled and more significantly from KhN55MBYU and KhN73MBTYu alloys (Fig. 1a). Increased effect of the hydrogen atmosphere was also found on aged specimens. High-nickel alloys are very noticeable in hydrogen at a pressure of 30 MPa. Thus, the relative elongation and the number of cycles to fracture of KhN62BMKTYu and KhN73MBTYu alloys decrease by six and about ten times, respectively (Table 2, Fig. 1b).

The joint effect of pre-absorbed and external hydrogen gas was assessed on several modifications of each studied material. They differ in chemical composition, modes of maintenance, to a small extent, strength characteristics in air and more significantly in the values of relative elongation, transverse narrowing, and low-cycle life, especially in the presence of hydrogen [11, 18–20, 23, 29–31]. The wide range of values of β coefficients for specimens from different modifications of all materials (Fig. 2) indicates that structural factors (grain size, number, morphology, and placement of secondary phases) play a significant role in hydrogen embrittlement. Atomic ordering with the formation of near-atomic order also increases hydrogen permeability and changes the hydrogen resistance of

steels [9, 48]. Under the same conditions of preliminary hydrogenation, the amount of absorbed hydrogen in high-nickel alloys is almost twice as high as in 05Kh11N23T3MR and 10Kh15N27T3V2MR austenitic steels (Table 2). The effect of hydrogen on the relative elongation of more hydrogen-resistant modifications of materials and low-cycle life increases with nickel content (Fig. 2a and 2c), and that on the relative transverse narrowing – remains almost stable in the range of 23–73 wt.% Ni (Fig. 2b). The degree of hydrogen embrittlement of various modifications of materials is significantly different in short-term tensile tests (Fig. 2a and 2b) and slightly less in low-cycle fatigue tests (Fig. 2c) when the number of cycles to failure is determined by the state of the surface of the specimens, where the maximum mechanical stresses and hydrogen concentrations are combined. A significant (1.6 times) weakening of the effect of hydrogen on low-cycle life was found only in the best modification of the KhN45MBTYu alloy (Fig. 2c). The difference in the values of the β_δ coefficient of 05Kh11N23T3MR steel modifications is more than 2-fold (Fig. 2a, Tables 2 and 3). Optimization of chemical composition and HT modes allows one to significantly (by 1.6 times) reduce the effect of hydrogen on the relative transverse narrowing of all materials (Fig. 2b) and the relative elongation of steels and alloys with nickel content up to 56% (Fig. 2a).

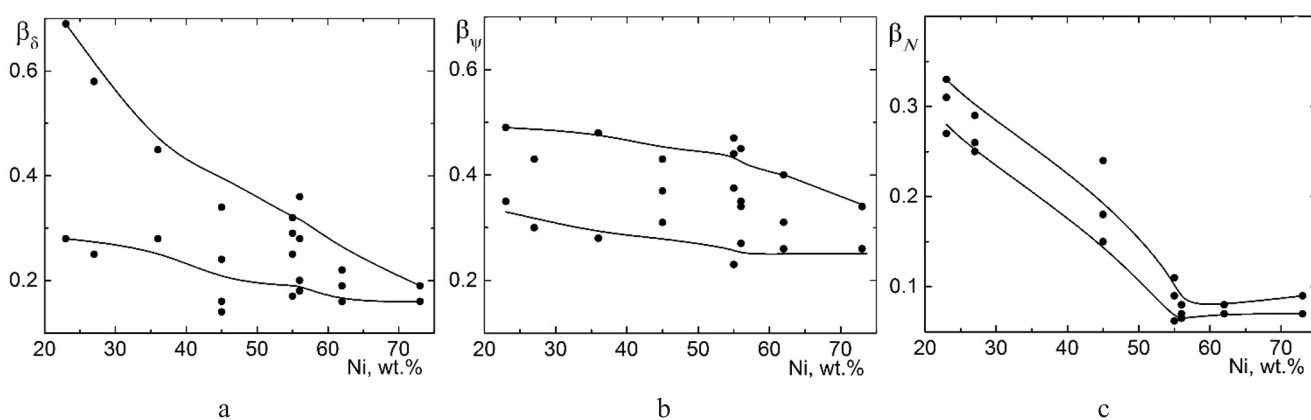


Fig. 2. Dependence of the coefficient of hydrogen effect β at a pressure of 30 MPa on the relative elongation δ (a), transverse narrowing ψ (b), and low-cycle life N (c) of pre-hydrogenated specimens of steels and alloys in the aged state on the nickel content at room temperature.

Only the modifications of materials presented in Tables 1 and 2 were tested at elevated temperatures. In the temperature range of 293–773 K, the effect of high-pressure hydrogen on the properties of pre-hydrogenated specimens made of 05Kh11N23T3MR and 10Kh15N27T3V2MR steels and KhN45MBTYu alloy is slightly weakened, and that of non-hydrogenated specimens is enhanced [18–20]. As a result, at temperatures above 773 K, when a sufficient amount of hydrogen for maximum hydrogen degradation penetrates the metal during short-term static tension, the plasticity of hydrogenated and non-hydrogenated specimens in a hydrogen environment is almost the same [18–20]. The additional effect of absorbed hydrogen on the properties of high-nickel alloys is insignificant in the temperature range of 293–1073 K [18–20]. Therefore, the dependences of the hydrogen embrittlement degree on the nickel content at 773 and 973 K are based on the test results of preliminary non-hydrogenated specimens (Fig. 3). At a temperature of 773 K, all materials retain a sufficiently high level of strength. The effect of nickel content on the coefficient β_ψ is slightly less but qualitatively the same as at 293 K (Fig. 2b and 3a). Increasing the temperature to 973 K leads to a decrease in strength and, accordingly, to the weakening of hydrogen embrittlement of 05Kh11N23T3MR and 10Kh15N27T3V2MR steels [18–20], therefore the effect of hydrogen on the plasticity of more heat-resistant high-nickel alloys is much stronger (Fig. 3b). The exception is the KhN55MBYU alloy with a smaller total amount of titanium, aluminum and niobium, i.e., intermetallic phase, and relatively low strength at elevated temperatures [18–20, 30]. Thus, at 973 K, the short-term tensile strength of this alloy is 620 MPa, of the KhN45MBTYu alloy is 750 MPa, and of the KhN56MBYuD and KhN62BMKTYu alloys is more than 1000 MPa.

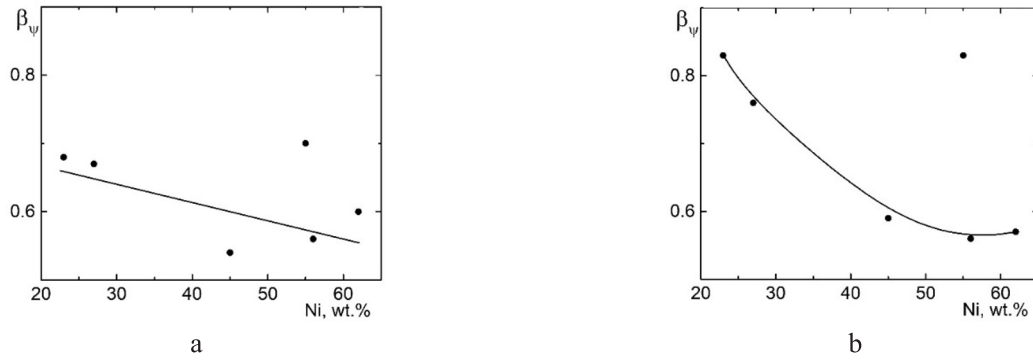


Fig. 3. Dependence of the coefficient of hydrogen effect β at a pressure of 30 MPa on the transverse narrowing ψ of specimens from steels and alloys in the aged state on the nickel content at a temperature of 773 (a) and 973 K (b).

Hydrogen causes a change in the fracture mechanism of specimens from ductile transcrystalline to intergranular fracture (Fig. 4), grinding of pits in the core of the specimen, where a small area of ductile fracture by tearing is preserved, and the nucleation of nanoscale voids at the grain boundaries and dislocation slip bands [18–20, 23, 24, 29–31, 39–43, 45–47]. Therefore, summarizing the results and literature data, it can be concluded that increasing the hydrogen resistance of austenitic iron-nickel steels and alloys is achieved by vacuum remelting [19, 30], reducing the amount of carbides and carbonitrides by minimizing the carbon content [2, 5, 18, 29–31, 39] (Tables 2 and 3), the formation of a structure with thin grain boundaries with increased cohesive energy by the introduction of boron, lanthanum, and zirconium [23, 29–31, 39–41], optimization of the morphology of intermetallics [21, 26, 32, 35]. Hydrogen embrittlement is weakened by copper alloying, which is especially effective in combination with the introduction of boron [37, 39]. The sensitivity to hydrogen and the number of intergranular fracture sites decrease with decreasing grain size, even though the hydrogen concentration in coarse-grained specimens is lower than in fine-grained ones [29, 30, 40]. Changing the grain size of the 30Ni-15Cr-1.3Mo-1.88Ti-0.36Al-0.24V-0.2Si-0.0008B-Fe alloy from 95 to 32 μm leads to the accumulation of a lower concentration of hydrogen at the grain boundaries since the number of dislocations in the slip bands that transport it is proportional to the grain size [21, 40].

TABLE 3. Treatment Modes and Mechanical Properties of the Investigated Materials at Room Temperature

| Processing mode | $\sigma_u/\sigma_u^1/\sigma_u^2$, MPa | $\sigma_{0.2}/\sigma_{0.2}^1/\sigma_{0.2}^2$, MPa | $\delta/\delta^1/\delta^2$, % | $\psi/\psi^1/\psi^2$, % |
|---|---|---|-----------------------------------|-----------------------------|
| 10Kh11N23T3MR | | | | |
| Quenching from 1373 K | 750/750/750 | 350/350/350 | 50/50/50 | 69/69/69 |
| Quenching from 1373 K, aging at 1000 K, 16 h + 923 K, 5 h | 1220/1190/1180 | 890/870/870 | 25/24/7 | 26/25/9 |
| Quenching from 1373 K, tensile stress 10%, 293 K + aging at 973 K, 16 h | 1210/1200/1190 | 890/890/890 | 24/24/16 | 28/28/16 |
| KhN45MBTYu | | | | |
| Quenching from 1373 K | 820/820/820 | 500/500/500 | 38/35/34 | 39/37/37 |
| Quenching from 1373 K, aging at 1023 K, 8 h + 923 K, 8 h | 1160/1130/960 | 780/780/740 | 25/22/4 | 38/30/14 |
| Quenching from 1473 K, aging at 1023 K, 8h + 923 K, 8h | 1180/980/990 | 770/760/760 | 21/13/3 | 24/16/8 |
| Quenching from 1473 K, tensile strength 7% at 293 K, aging at 973 K, 16 h | 1260/1210/1200 | 820/820/820 | 24/22/16 | 46/40/28 |

Note. σ_u , $\sigma_{0.2}$, δ , ψ are properties in air; σ_u^1 , $\sigma_{0.2}^1$, δ^1 , ψ^1 are properties in hydrogen at 30 MPa; σ_u^2 , $\sigma_{0.2}^2$, δ^2 , ψ^2 are properties in hydrogen at 30 MPa after hydrogenation.

One of the methods for obtaining a combination of high strength, plasticity, and hydrogen resistance of stainless austenitic chromium-nickel and chromium-manganese-nickel steels [13, 49] and heat-resistant nickel alloys [25, 33] is thermomechanical treatment (TMT). After three cycles of cold rolling followed by 15-min annealing at 1173 K in an air furnace, specimens of technically pure nickel at hydrogen concentrations of more than 20 ppm⁻¹ almost doubled the tensile plasticity, the proportion of intergranular fracture became much lower, and the value of J_c fracture toughness was about 20–30% higher [50].

The effectiveness of TMT (quenching, tensile at 5, 7, and 10% at room temperature and aging for 16 h at 973 K) was assessed on the modifications of 10Kh11N23T3MR steel and KhN45MBTYu alloy. They differed from those indicated in Tables 1 and 2 by the carbon content of 0.097 wt.% (10Kh11N23T3MR steel) and higher quenching temperature, i.e., coarser grain structure (KhN45MBTYu alloy) (Table 3). The hydrogen content in the pre-hydrogenated aged specimens practically did not depend on the processing mode, as indicated in Table 2.

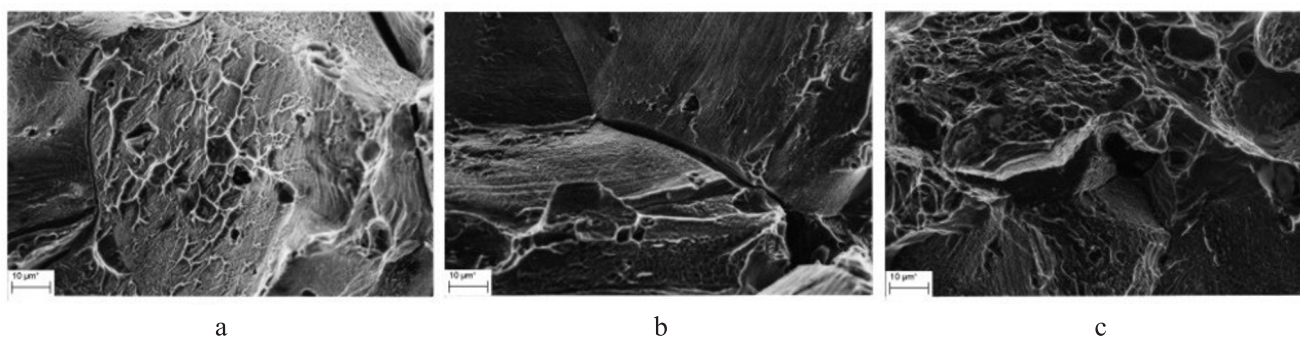


Fig. 4. Fracture pattern of specimens made of 10Kh11N23T3MR steel: (a) air, HT; (b) hydrogen, HT; (c) hydrogen, TMT.

The external hydrogen environment does not deteriorate the properties of 10X11H23T3MP steel regardless of chemical composition and processing mode (Tables 2 and 3, Figs. 1 and 2). The structural state of the material significantly determines its hydrogen resistance under the combined action of external and pre-absorbed hydrogen. High resistance to hydrogen embrittlement in this test mode is typical only for the hardened material, in which the amount of intermetallic γ' -phase is insignificant (Table 3). An increase in the carbon content in the aged specimens of 10Kh11N23T3MR steel from 0.05 to 0.097 wt.% had a weak effect on their strength. It led to a decrease in plasticity, especially significant when tested in the presence of hydrogen (Tables 2 and 3). Under the same aging mode, the plasticity of KhN45MBTYu alloy specimens with coarse grains, when the intermetallic γ' -phase was concentrated mainly on the grain boundaries [51], decreased under all conditions of hydrogen exposure more significantly than that of specimens with a fine-grained structure (Table 3). TMT significantly increased the hydrogen resistance of materials. Thus, at the optimum deformation degree, which for 10Kh11N23T3MR steel was equal to 10%, the strength properties of steel after TMT and step aging were the same, and the relative elongation of hydrogenated specimens increased from 7% (HT) to 16% (TMT), i.e., more than twice (Table 3). The size and number of discharges at the grain boundaries and, accordingly, the proportion of intergranular fracture in the fracture of hydrogenated specimens decreased markedly (Fig. 4). The combination of high strength and plasticity of both non-hydrogenated and pre-hydrogenated specimens from more alloyed alloy KhN45MBTYu during tests in hydrogen at a pressure of 30 MPa was achieved after TMT with the tensile strength of 7%, i.e., such treatment was effective under the action of external and absorbed hydrogen.

The increased resistance to hydrogen embrittlement after TMT was due to the following reasons. Firstly, since the γ' -phase particles released at the grain boundaries, due to interfacial stresses contributed to the segregation of hydrogen there, the reduction of their number and size [51] improved the hydrogen resistance of alloys. Secondly, dispersed dislocations in the grain body acted as barriers to mobile dislocations and hydrogen traps, reducing

hydrogen transport efficiency to grain boundaries. Consequently, a more uniform distribution of particles of strengthening phases promoted a similar distribution of hydrogen, weakening its effect on mechanical properties.

CONCLUSIONS

1. The influence of gaseous hydrogen at a pressure of 30 MPa and room temperature on the plasticity characteristics and low-cycle life of hardened iron-nickel steels and alloys decreases with increasing nickel concentration from 10 to 23 wt.%, is insignificant in the concentration range of 23–45 wt.%, and significantly increases with higher nickel content. After aging, materials with 23 and 36 wt.% nickel are insensitive to the hydrogen environment; at higher concentrations, embrittlement increases and becomes very noticeable in alloys with 55, 62, and 73 wt.% nickel when the listed characteristics decrease more than five times.

2. Under the same conditions of preliminary hydrogenation, the amount of absorbed hydrogen in high-nickel alloys is almost twice as high as in austenitic steels. The structural state of hydrogenated materials significantly affects the degree of hydrogen embrittlement of their various modifications in short-term tensile tests and slightly less in low-cycle fatigue tests. In the interval of Ni concentrations of 23–73 wt.%, the effect of hydrogen on the relative transverse narrowing remains almost stable, and on the relative elongation of more hydrogen-resistant modifications of materials and low-cycle life increases with increasing nickel content.

3. At elevated temperatures, the effect of nickel content is associated with the temperature dependencies of the strength of materials. At 773 K, all steels and alloys retain a sufficiently high level of strength characteristics. The effect of nickel content on the coefficient β_{ψ} in gaseous hydrogen at a pressure of 30 MPa is slightly less. Still, qualitatively the same as at 293 K. Increasing the temperature to 973 K leads to a decrease in strength and, accordingly, to a weakening of hydrogen embrittlement of steels. Hence, the effect of hydrogen on the plasticity of more heat-resistant high-nickel alloys is much stronger.

4. Thermomechanical treatment according to the quenching scheme, tension at room temperature, and aging for 16 h at 973 K leads to a decrease in the size and number of discharges at the grain boundaries, the proportion of intergranular fracture in the fracture of hydrogenated specimens and, accordingly, to an increase in the plasticity of materials in the presence of hydrogen. At the optimum degree of deformation, which for steel 10Kh11N23T3MR is equal to 10%, the strength properties of steel after TMT and step aging are the same, and the relative elongation of hydrogenated specimens increased from 7% (HT) to 16% (TMT). The combination of high strength and ductility of specimens made of KhN45MBTYu alloy when tested in hydrogen at a pressure of 30 MPa is achieved after TMO with a tensile strength of 7%. Such treatment is effective under the action of external and absorbed hydrogen.

REFERENCES

1. R. P. Gangloff and B. P. Somerday, *Gaseous Hydrogen Embrittlement of Materials in Energy Technologies, Vol. 1: The Problem, Its Characterisation and Effects on Particular Alloy Classes*, Woodhead Publishing Limited, Cambridge, UK (2012).
2. M. Dadfarnia, A. Nagao, S. Wang, et al., “Recent advances on hydrogen embrittlement of structural materials,” *Int J Fracture*, **196**, 223–243 (2015).
3. A. V. Fishgoit and B. A. Kolachev, “Strength tests in hydrogen in the aerospace industry,” *Mater Sci*, **33**, No. 4, 568–573 (1997).
4. R. P. Gangloff, “Science-based prognosis to manage structural alloy performance in hydrogen,” in: B. Somerday, P. Sofronis, and J. Russell (Eds.), *Effects of Hydrogen on Materials* (Proc. of the 2008 International Hydrogen Conference, Wyoming), ASM International, Materials Park, USA (2009), pp. 1–21.
5. A. Lee, “Hydrogen embrittlement of nickel, cobalt and iron-based superalloys,” in: R.P. Gangloff and B.P. Somerday (Eds.), *Gaseous Hydrogen Embrittlement of Materials in Energy Technologies: The Problem, Its Characterization, and Effects on Particular Alloy Classes*, Woodhead Publishing Limited, Cambridge, UK (2012), pp.624–667.

6. T. Michler, J. Naumann, and M. P. Balogh, "Hydrogen environment embrittlement of solution treated Fe–Cr–Ni superalloys," *Mater Sci Eng A*, **607**, 71–80 (2014).
7. F. Galliano, E. Andrieu, C. Blanc, et al., "Effect of trapping and temperature on the hydrogen embrittlement susceptibility of alloy 718," *Mater Sci Eng A*, **611**, 370–382 (2014).
8. T. Michler, J. Naumann, J. Wiebesiek, et al., "Influence of frequency and wave form on S-N fatigue of commercial austenitic stainless steels with different Nickel contents in inert gas and in high pressure gaseous hydrogen," *Int J Fatigue*, **96**, 67–77 (2017).
9. V. G. Gavriljuk, V. Shyvaniuk, and S. Teus, "Hydrogen embrittlement," in: *Hydrogen in Engineering Metallic Materials*, Springer, Cham (2022), pp. 201–274.
10. S. Brück, V. Schippl, M. Schwarz, et al., "Hydrogen embrittlement mechanism in fatigue behavior of austenitic and martensitic stainless steels," *Metals*, **8**, No. 5, 339 (2018).
11. G. G. Maksimovich, I. Yu. Tretyak, L. M. Ivas'kevich, et al., "Role of the martensite transformation in hydrogen embrittlement of unstable austenitic steels," *Sov Mater Sci*, **21**, No. 4, 320–323 (1986).
12. V. I. Vitvitskii, V. I. Tkachev, M. F. Berezhnitskaya, et al., "Assessment of mechanical properties and phase-structural state in corrosion-resistant steels under static and low-cycle loading," *Strength Mater*, **39**, No. 5, 466–474 (2007). <https://doi.org/10.1007/s11223-007-0052-y>
13. H. Zhang, J. Hud, and X. Meng, "Effect of deformation microstructures on hydrogen embrittlement sensitivity and failure mechanism of 304 austenitic stainless steel: the significant role of rolling temperature," *J Mater Res Technol*, **17**, 2831–2846 (2022).
14. Y. Murakami, T. Kanezaki, and Y. Mine, "Hydrogen embrittlement mechanism in fatigue of austenitic stainless steels," *Met Mater Trans A*, **39**, 1327–1339 (2008).
15. C. S. Marchi, T. Michler, K. A. Nibura, et al., "On the physical differences between tensile testing of type 304 and 316 austenitic stainless steels with internal hydrogen and in external hydrogen," *Int J Hydrogen Energ*, **35**, No. 18, 9736–9745 (2010).
16. D. M. Symons, "A comparison of internal hydrogen embrittlement and hydrogen environment embrittlement of X-750," *Eng Fract Mech*, **68**, No. 6, 751–771 (2001).
17. Y. Ogawa, H. Hosoi, K. Tsuzaki, et al., "Hydrogen, as an alloying element, enables a greater strength-ductility balance in an Fe-Cr-Ni-based, stable austenitic stainless steel," *Acta Mater*, **199**, 181–192 (2020).
18. A. I. Balitskii and L. M. Ivaskevich, "Assessment of hydrogen embrittlement in high-alloy chromium-nickel steels and alloys in hydrogen at high pressures and temperatures," *Strength Mater*, **50**, No. 6, 880–887 (2018). <https://doi.org/10.1007/s11223-019-00035-2>
19. A. Balitskii, L. Ivaskevich, V. Mochul'skiy, et al., "Influence of high pressure and high temperature hydrogen on fracture toughness of Ni-containing steels and alloys," *Arch Mech Eng*, **61**, No. 1, 129–138 (2014).
20. V. I. Tkachov, L. M. Ivas'kevych, and V. M. Mochul's'kiy, "Temperature dependences of the mechanical properties of austenitic and martensitic steels in hydrogen," *Mater Sci*, **43**, No. 5, 654–666 (2007).
21. J. E. Smugeresky, "Effect of hydrogen on the mechanical properties of iron-base superalloys," *Metall Trans A*, **8**, No. 8, 1283–1289 (1977).
22. J. A. Brooks and M. R. Louthan, "Surface preparation and hydrogen compatibility of an iron base superalloy," *Metall Trans A*, **11**, No. 12, 1981–1986 (1980).
23. A. I. Balitskii, L. M. Ivaskevich, and V. M. Mochul'skiy, "Crack resistance of age-hardening Fe-Ni alloys in gaseous hydrogen," in: Proc. on CD ROM of the 18th Europ. Conf. on Fracture. Fracture of Materials and Structures from Micro to Macro Scale, (Dresden, Germany, Sept. 2010). Code 93905.
24. O. Takakuwa, Y. Ogawa, J. Yamabe, et al., "Hydrogen-induced ductility loss of precipitation-strengthened Fe-Ni-Cr-based superalloy," *Mater Sci Eng A*, **739**, 335–342 (2019).
25. M. S. Hazarabedian and M. Iannuzzi, "The role of nano-sized intergranular phases on nickel alloy 725 brittle failure," *npj Mater Degrad*, **5**, No. 1, Article ID 39 (2021).

26. Z. Zang, G. Obasi, R. Morana, et al., “In-situ observation of hydrogen induced crack initiation in a nickel-based superalloy,” *Scripta Mater*, **140**, 40–44 (2017).
27. P. D. Hicks and C. J. Altstetter, “Hydrogen-enhanced cracking of superalloys,” *Metall Mater Trans A*, **23**, No. 1, 237–249 (1992).
28. T. Michler, “Influence of gaseous hydrogen on the tensile properties of Fe-36Ni INVAR alloy,” *Int J Hydrogen Energ*, **39**, No. 22, 11807–11809 (2014).
29. O. I. Balyts’kyi, L. M. Ivas’kevych, and J. J. Elias, “Static crack resistance of heat-resistant KhN43MBTYu nickel-chromium alloy in gaseous hydrogen,” *Strength Mater*, **52**, No. 3, 386–397 (2020). <https://doi.org/10.1007/s11223-020-00189-4>
30. A. I. Balitskii and L. M. Ivaskevich, “Hydrogen effect on cumulation of failure, mechanical properties, and fracture toughness of Ni-Cr alloys,” *Adv Mater Sci Eng*, **2019**, 3680253 (2019).
31. O. I. Balyts’kyi, V. M. Mochyl’skyi, and L. M. Ivas’kevych, “Evaluation of the influence of hydrogen on mechanical characteristics of complexly alloyed nickel alloys,” *Mater Sci*, **51**, No. 4, 538–547 (2016).
32. M. C. Rezende, L. S. Araujo, S. B. Gabriel, et al., “Hydrogen embrittlement in nickel-based superalloy 718: Relationship between $\gamma' + \gamma''$ precipitation and the fracture mode,” *Int J Hydrogen Energ*, **40**, No. 47, 17075–17083 (2015).
33. X. Lu, Y. Ma, and D. Wang, “On the hydrogen embrittlement behavior of nickel-based alloys: alloys 718 and 725,” *Mater Sci Eng A*, **792**, 139785 (2020).
34. V. I. Tkachov, I. M. Levina, and L. M. Ivas’kevych, “Distinctive features of hydrogen hydrogen degradation of heat-resistance alloys based on nickel,” *Mater Sci*, **33**, No. 4, 524–531 (1997).
35. Y. Ogawa, K. Noguchi, and O. Takakuwa, “Criteria for hydrogen-assisted crack initiation in Ni-based superalloy 718,” *Acta Mater*, **229**, 117789 (2022).
36. Z. D. Harris, J. J. Bhattacharyya, J. A. Ronevich, et al., “The combined effects of hydrogen and aging condition on the deformation and fracture behavior of a precipitation-hardened nickel-base superalloy,” *Acta Mater*, **186**, 616–630 (2020).
37. N. A. Sorokina, T. K. Sergeeva, Yu. I. Rusinovich, et al., “Hydrogen embrittlement resistance of differently doped nickel alloys,” *Fiz.-Khim. Mekh. Mater.*, **21**, No. 1, 27–31 (1985).
38. I. Taji, T. Hajilou, S. Karimi, et al., “Role of grain boundaries in hydrogen embrittlement of alloy 725: single and bi-crystal microcantilever bending study,” *Int J Hydrogen Energ*, **47**, No. 25, 12771–12781 (2022).
39. I. Taji, T. Hajilou, A. S. Jelinek, et al., “Hydrogen assisted intergranular cracking of alloy 725: the effect of boron and copper alloying,” *Corros Sci*, **203**, 110331 (2022).
40. S. Chen, M. Zhao, and L. Rong, “Effect of grain size on the hydrogen embrittlement sensitivity of a precipitation strengthened Fe-Ni based alloy,” *Mater Sci Eng A*, **594**, 98–102 (2014).
41. D.-H. Lee, Y. Zhao, S. Y. Lee, et al., “Hydrogen-assisted failure in Inconel 718 fabricated by laser powder bed fusion: The role of solidification substructure in the embrittlement,” *Scripta Mater*, **207**, 114308 (2022).
42. H. Chen, Y. Ma, C. Li, et al., “A nano-sized NbC precipitation strengthened FeCoCrNi high entropy alloy with superior hydrogen embrittlement resistance,” *Corros Sci*, **208**, 110636 (2022).
43. Z. Zhang, G. Obasi, R. Morana, et al., “Hydrogen assisted crack initiation and propagation in a nickel-based superalloy,” *Acta Mater*, **113**, 272–283 (2016).
44. J. H. Holbrook, H. J. Cialone, E. W. Collins, et al., “Control of hydrogen embrittlement of metals by chemical inhibitors and coatings,” in: R. P. Gangloff and B. P. Somerday (Eds.), *Gaseous Hydrogen Embrittlement of Materials in Energy Technologies*, Vol. 2: *Mechanisms, Modeling and Future Developments*, Woodhead Publishing Limited, Cambridge, UK (2012), pp. 129–153.
45. I. M. Dmytrakh, A. M. Syrotyuk, and R. L. Leshchak, “Effect of preliminary hydrogenation–dehydrogenation of low-alloy steel on its ability to absorb electrochemical hydrogen,” *Mater Sci*, **57**, No. 3, 387–396 (2021).

46. A. M. Syrotyuk and I. M. Dmytrakh, "Methods for the evaluation of fracture and strength of pipeline steels and structures under the action of working media. Part II. Influence of hydrogen-containing media," *Mater Sci*, **50**, No. 4, 475–487 (2015).
47. V. I. Pokhmurskii, V. V. Fedorov, P. N. Antonevich, et al., "Variation of the phase and structural state of ÉP-838 and 316SS alloys in interaction with hydrogen," *Sov Mater Sci*, **23**, No. 6, 572–576 (1987).
48. M. G. Stashchuk, "Microcracks on the continuation of the dislocation nucleus," *Fiz.-Khim. Mekh. Mater.*, **58**, No. 2, 95–102 (2022).
49. V. I. Tkachov and L. M. Ivas'kevych, "Mechanical properties of chromium-manganese austenite steels in a hydrogen environment," *Mater Sci*, **35**, No. 5, 684–688 (1999).
50. S. Bechtle, M. Kumar, B. P. Somerday, et al., "Grain-boundary engineering markedly reduces susceptibility to intergranular hydrogen embrittlement in metallic materials," *Acta Mater*, **57**, 4148–4157 (2009).
51. C. Sims and W. Hagel, *Heat-Resistant Alloys* [Russian translation], Metallurgiya, Moscow (2004).